Tailoring Nanoadsorbent Surfaces for Recycling of LTM

Subjects: Nanoscience & Nanotechnology

Contributor: Gulaim A. Seisenbaeva , Ani Vardanyan ,

A series of adsorbents were tailored for selective extraction of rare earth elements (REE) and late transition metals (LTM) via grafting of ligands bearing specific N- and S-donor functions. All obtained adsorbents showed relatively quick uptake kinetics and high adsorption capacity 0.5 to 1.8 mmol/g, depending on the function and the target metal ion. The adsorption equilibrium data analyzed and fitted well to Langmuir isotherm model revealing monolayer adsorption process on homogeneously functionalized silica nanoparticles (NPs). Most of the employed ligands demonstrated higher affinity towards LTM compared to REE, related to the nature of the functional groups and their arrangement on the surface of nanoadsorbent.

recycling silica nanoadsorbents adsorption REE LTM

1. Introduction

During the past few decades, there has been a continuous increase in the applications of Rare Earth Elements (REE) and their alloys, making them critical elements for development of modern industries [1]. The main target markets using REEs include magnets, metallurgy, catalysts, polishing powders, batteries, mobile phones and other high-technology gadgets. With their growing demand and continuous supply risk, urban mining of REEs from different end-of-life products and industrial waste has gained increasing attention [2]. As such, permanent magnets, which have various applications in the development of new technological devices as well as for green energy production, are one of the most promising secondary sources of REEs that can be recycled and reused [3]. Common Rare Earth-based magnets include Neodymium–iron–boron (FeNdB) and Samarium–cobalt (SmCo) magnets [4]. One of the key challenges in the recycling of magnet materials lies in the need to separate REE from Late Transition Metals (LTM), which form their constituents or major materials of their casings [5]. The most common technology for REE separation is acidic leaching with different leaching agents such as hydrochloric and sulfuric acids [6][7]. Iron is the major component in FeNdB and in the casing of magnets in electronics. It needs to be removed in the step previous to the separation of all other components, for both economic and technical reasons. The well-established approaches for separation of iron from leachates include either precipitation of iron hydroxide during controlled elevation of pH [8] or the precipitation of all other components apart from iron by addition of oxalic acid and organic base [9]. The precipitate can then be calcined and re-dissolved in acid. Subsequent separation of the components can be achieved by solvent extraction, ion exchange, or adsorption [10]. Most of the established industrial methods require, however, repeated steps to obtain the desired purity, thus generating large amounts of hazardous and, in the case of primary ore treatment, even radioactive waste [11][12]. As an alternative to the

traditionally used methods, the application of solid-phase extraction (SPE) using nanosized functional adsorbents has been proven to be an effective and more environmentally friendly method for REE recovery [13]. Various types of nanosorbents have been synthesized for SPE recovery of REEs [14][15][16][17][18][19][20][21]. Several reviews have already been devoted to the discussion of the advantages and challenges in the application of functional solid adsorbents for REE separation [22][23]. Recent works have shown that organic–inorganic functionalized silica nanoparticles possess great adsorption capacity and selectivity towards many metal ions, including heavy metals and REEs [24]. Functional groups such as iminodiacetic acid (IDA), diethylenetriaminepentaacetic acid (DTPA), ethylenediaminetetraacetic acid (EDTA) and triethylenetetraminehexaacetic acid (TTHA) were grafted on dense SiO_2 nanoparticles as well as SiO_2 core–shell magnetic nanoparticles and tested for different REEs adsorption and separation. High adsorption capacities of up to 300 mg of RE^{3+}/g were reached, and distinct selectivity trends towards different REEs depending on the complexonate [25][26][27].

The majority of earlier successfully applied ligands belonged to the classes of either complexons, i.e., amino carboxylic acids [28], or crown ethers/cyclenes. These types of ligands revealed strong affinity to both REE and LTM. In this entry, the new ligands (N-(2-Aminoethyl)-3-aminopropyltrimethoxysilane **L1** and N-(2-Aminoethyl)-3-AminoIsobutylmethyl Dimethoxysilane **L4**—a derivative of ethylene diamine, known for high affinity to Ni^{2+} and Cu^{2+} and, to a lesser extent, for Co^{2+} [29][30][31]; 2-(2-Pyridilethyl) Thiopropyltrimethoxysilane **L2**—a derivative of pyridine with potentially good affinity to LTM and also a sulfur bridge [32][33]; and Triethoxy(3-isothiocyanatopropyl)silane **L3** and Triethoxy(3-thiocyanatopropyl)silane **L5**—derived from isothiocyanate with potential affinity to Ni^{2+} and Co^{2+} [34], were selected and grafted on SiO_2 nanoparticles to achieve selectivity for separating LTM from REEs in mixed solutions (**Figure 1**).

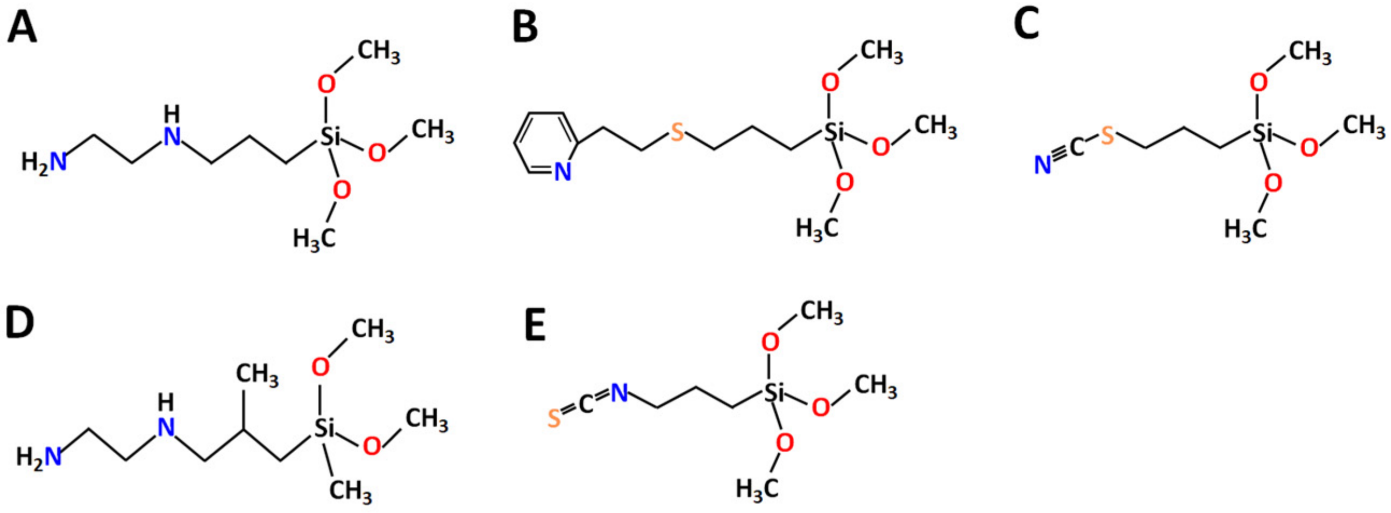

Figure 1. Chemical structure of selected ligands: (**A**) **L1**, (**B**) **L2**, (**C**) **L3**, (**D**) **L4** and (**E**) **L5**.

2. Adsorption Equilibrium Isotherms

The effect of the concentrations of LTM (Co and Ni) and of RE^{3+} (Nd and Sm) on adsorption efficiency was investigated in batch studies at room temperature. The results showed that the adsorbed amount of metal ions on

grafted SiO_2 NPs increased with increasing the initial metal concentration and reached to the maximum adsorption capacity at higher concentrations due to saturation of the binding sites (**Figure 2**). The maximum adsorption capacities are summarized in **Table 1**. Based on the results, **SiO_2_L1** demonstrated higher adsorption capacities for all LTM and REEs, which is in agreement with TGA results, considering the grafted amount of the ligands per unit mass of SiO_2 NPs was higher compared to **SiO_2_L2** and **SiO_2_L3**. SiO_2 with both **L2** and with **L3** had similar maximum adsorption capacities for most of the metal ions, only for Co adsorption did SiO_2 NPs grafted with **L3** ligands demonstrate a slightly higher adsorption capacity. However, acid-treated SiO_2 with **L3** (**SiO_2_L3_acid**) and **L5** (**SiO_2_L5_acid**) showed improved adsorption by increasing their maximum capacities by twice for Co, Nd, Sm, and by almost five times in the case of Ni. According to the literature, sulfur- and amine-containing groups possess higher selectivity towards LTM, which can explain the higher adsorption capacities towards Ni and Co for most of these ligands [35][36][37][38][39][40].

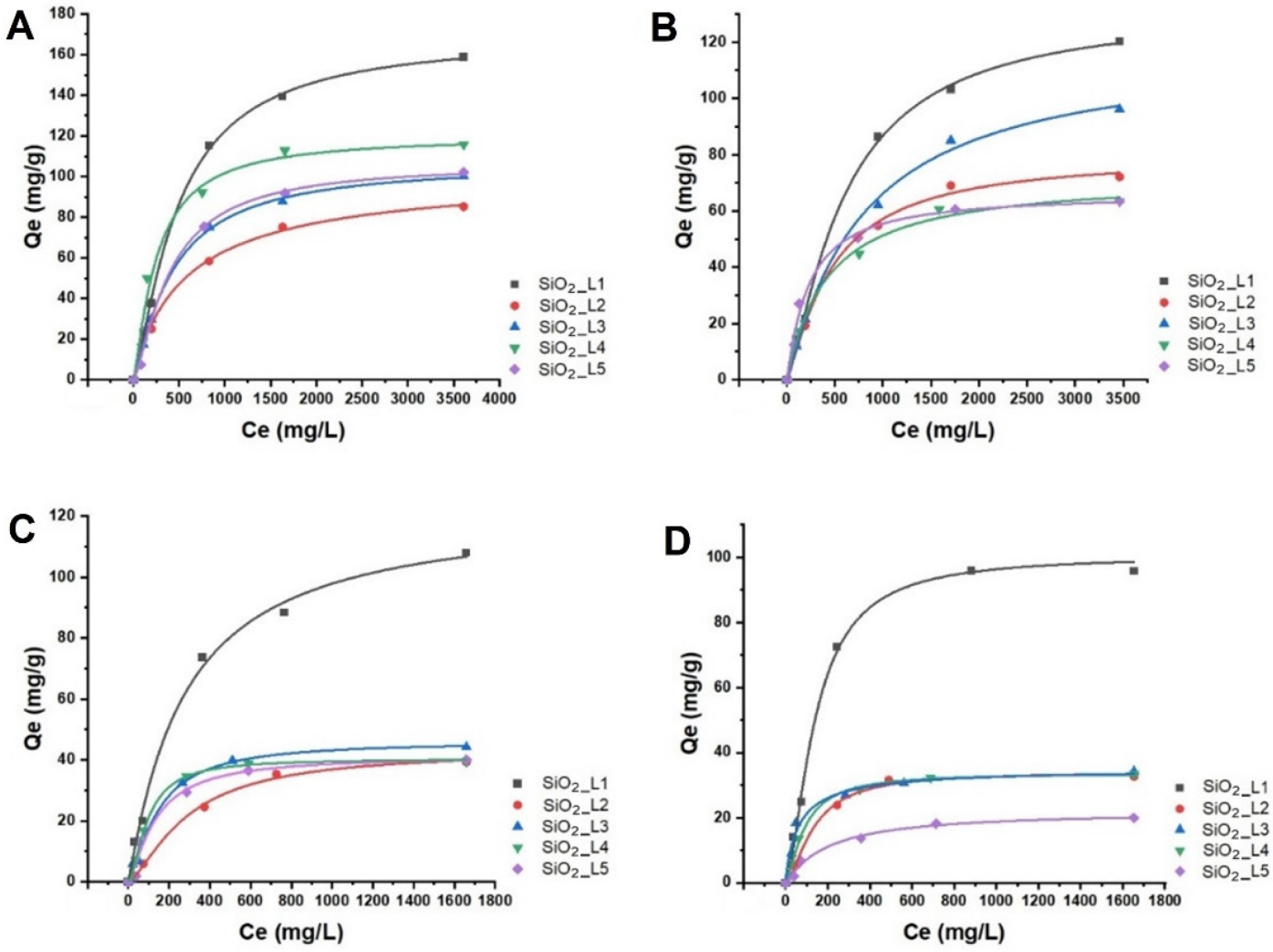

Figure 2. Langmuir adsorption isotherms of (**A**) Sm, (**B**) Nd, (**C**) Co and (**D**) Ni ions onto functionalized silica nanoparticles.

Table 1. Maximum adsorption capacities of grafted SiO_2 NPs towards REEs and LTM.

Sample	Ni (mmol/g)	Co (mmol/g)	Nd (mmol/g)	Sm (mmol/g)
SiO_2_L1	1.66	1.83	0.83	1.10
SiO_2_L2	0.55	0.66	0.50	0.56
SiO_2_L3	0.58	0.75	0.67	0.66
SiO_2_L4	0.57	0.67	0.44	0.77
SiO_2_L5	0.34	0.68	0.44	0.68
SiO_2_L3_acid	1.00	1.33	0.75	0.83
SiO_2_L5_acid	1.66	1.33	0.75	1.00

References

1. Balaram, V. Rare earth elements: A review of applications, occurrence, exploration, analysis, recycling, and environmental impact. Geosci. Front. 2019, 10, 1285–1303.
2. Mancheri, N.A.; Sprecher, B.; Bailey, G.; Ge, J.; Tukker, A. Effect of Chinese policies on rare earth supply chain resilience. Resour. Conserv. Recycl. 2019, 142, 101–112.
3. Yang, Y.; Walton, A.; Sheridan, R.; Güth, K.; Gauß, R.; Gutfleisch, O.; Buchert, M.; Steenari, B.M.; ...net ...m-iron ...n and ...s Using ...im, J.G. ...t. ...rocess for neodymium recovery from scrap Nd-Fe-B magnet. Metall. Mater. Trans. A Phys. Metall. Mater. Sci. 2013, 44, 5825–5833.
8. Seisenbaeva, G.A.; Legaria, E.P.; Kessler, V. Separation of Rare Earth Elements from Other Elements. US Patent 10787722, 29 September 2020.
9. Prodius, D.; Klocke, M.; Smetana, V.; Alammar, T.; Perez Garcia, M.; Windus, T.L.; Nlebedim, I.C.; Mudring, A.V. Rationally designed rare earth separation by selective oxalate solubilization. Chem. Commun. 2020, 56, 11386–11389.

Better insights into the mechanisms of adsorption require application of structure-sensitive characterization techniques. In the present work, researchers recorded calibrated UV-Vis spectra of adsorbents before and after uptake of LTM. The spectra reveal a distinct shift of the adsorption maximum for the Co^{2+}-derived materials, indicating that uptake of this cation presumably proceeds via formation of inner-sphere complexes with surface ligands. An image demonstrating the potential binding geometry is provided. More detailed insight into coordination of adsorbed cations would require more in-depth investigation with techniques such as, for example, X-ray absorption spectroscopy, applying well-defined structural models from X-ray diffraction studies of relevant model compounds, and will be reported separately later.

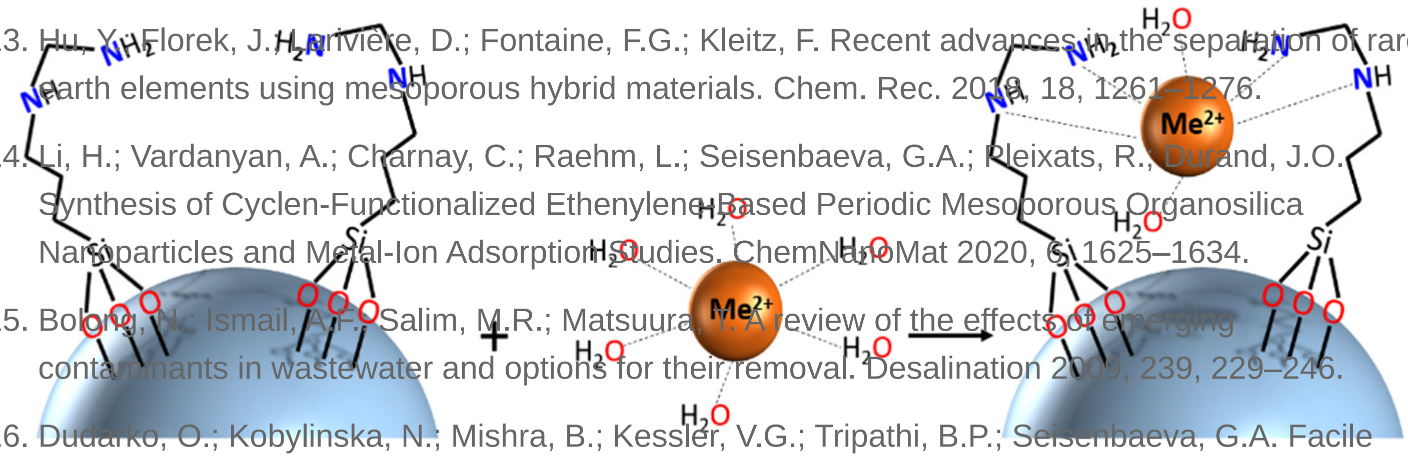

Scheme 1. Schematic representation of potential binding mechanism of **SiO_2-L1** with metal cations.

The adsorption kinetics showed that most of the uptake (60–80%) occurred within the first 1–2 h of interaction of metals with silica nanoparticles. Slower adsorption continues, and equilibrium is reached after 3–5 h (**Figure 3**).

10. Li, C.; Ramasamy, D.L.; Sillanpää, M.; Repo, E. Separation and concentration of rare earth elements from wastewater using electrodialysis technology. Sep. Purif. Technol. 2021, 254, 117442.

11. Wang, Y.; Huang, C.; Li, F.; Dong, Y.; Sun, X. Process for the separation of thorium and rare earth elements from radioactive waste residues using Cyanex® 572 as a new extractant. Hydrometallurgy 2017, 169, 158–164.

12. García, A.C.; Latifi, M.; Amini, A.; Chaouki, J. Separation of radioactive elements from rare earth element-bearing minerals. Metals 2020, 10, 1524.

13. Hu, Y.; Florek, J.; Larivière, D.; Fontaine, F.G.; Kleitz, F. Recent advances in the separation of rare earth elements using mesoporous hybrid materials. Chem. Rec. 2018, 18, 1261–1276.

14. Li, H.; Vardanyan, A.; Charnay, C.; Raehm, L.; Seisenbaeva, G.A.; Pleixats, R.; Durand, J.O. Synthesis of Cyclen-Functionalized Ethenylene-Based Periodic Mesoporous Organosilica Nanoparticles and Metal-Ion Adsorption Studies. ChemNanoMat 2020, 6, 1625–1634.

15. Bolong, N.; Ismail, A.F.; Salim, M.R.; Matsuura, T. A review of the effects of emerging contaminants in wastewater and options for their removal. Desalination 2009, 239, 229–246.

16. Dudarko, O.; Kobylinska, N.; Mishra, B.; Kessler, V.G.; Tripathi, B.P.; Seisenbaeva, G.A. Facile strategies for synthesis of functionalized mesoporous silicas for the removal of rare-earth elements and heavy metals from aqueous systems. Microporous Mesoporous Mater. 2021, 315, 110919.

17. Shyam Sunder, G.S.; Rohanifar, A.; Alipourasiabi, N.; Lawrence, J.G.; Kirchhoff, J.R. Synthesis and Characterization of Poly(pyrrole-1-carboxylic acid) for Preconcentration and Determination of Rare Earth Elements and Heavy Metals in Water Matrices. ACS Appl. Mater. Interfaces 2021, 13, 34782–34792.

18. Seisenbaeva, G.A.; Ali, L.M.A.; Vardanyan, A.; Gary-Bobo, M.; Budnyak, T.M.; Kessler, V.G.; Durand, J.O. Mesoporous silica adsorbents modified with amino polycarboxylate ligands—Functional characteristics, health and environmental effects. J. Hazard. Mater. 2021, 406, 124698.

19. Ashour, R.M.; Samouhos, M.; Polido Legaria, E.; Svärd, M.; Högblom, J.; Forsberg, K.; Palmlöf, M.; Kessler, V.G.; Seisenbaeva, G.A.; Rasmuson, Å.C. DTPA-Functionalized Silica Nano- and Microparticles for Adsorption and Chromatographic Separation of Rare Earth Elements. ACS Sustain. Chem. Eng. 2018, 6, 6889–6900.

20. Florek, J.; Larivière, D.; Kählig, H.; Fiorilli, S.L.; Onida, B.; Fontaine, F.G.; Kleitz, F. Understanding Selectivity of Mesoporous Silica-Grafted Diglycolamide-Type Ligands in the Solid-Phase Extraction of Rare Earths. ACS Appl. Mater. Interfaces 2020, 12, 57003–57016.

21. Abdel-Magied, A.F.; Abdelhamid, H.N.; Ashour, R.M.; Zou, X.; Forsberg, K. Hierarchical porous zeolitic imidazolate frameworks nanoparticles for efficient adsorption of rare-earth elements. Microporous Mesoporous Mater. 2019, 278, 175–184.
22. Kegl, T.; Košak, A.; Lobnik, A.; Novak, Z.; Kralj, A.K.; Ban, I. Adsorption of rare earth metals from wastewater by nanomaterials: A review. J. Hazard. Mater. 2020, 386, 121632.
23. Asadollahzadeh, M.; Torkaman, R.; Torab-Mostaedi, M. Extraction and Separation of Rare Earth Elements by Adsorption Approaches: Current Status and Future Trends. Sep. Purif. Rev. 2020, 50, 417–444.
24. Kobylinska, N.; Dudarko, O.; Kessler, V.; Seisenbaeva, G. Enhanced removal of Cr (III), Mn (II), Cd (II), Pb (II) and Cu (II) from aqueous solution by N-functionalized ordered silica. Chem. Afr. 2021, 4, 451–461.
25. Topel, S.D.; Legaria, E.P.; Tiseanu, C.; Rocha, J.; Nedelec, J.M.; Kessler, V.; Seisenbaeva, G.A. Hybrid silica nanoparticles for sequestration and luminescence detection of trivalent rare-earth ions (Dy3+ and Nd3+) in solution. J. Nanoparticle Res. 2014, 16, 2783.
26. Polido Legaria, E.; Samouhos, M.; Kessler, V.G.; Seisenbaeva, G.A. Toward Molecular Recognition of REEs: Comparative Analysis of Hybrid Nanoadsorbents with the Different Complexonate Ligands EDTA, DTPA, and TTHA. Inorg. Chem. 2017, 56, 13938–13948.
27. Ramasamy, D.L.; Khan, S.; Repo, E.; Sillanpää, M. Synthesis of mesoporous and microporous amine and non-amine functionalized silica gels for the application of rare earth elements (REE) recovery from the waste water-understanding the role of pH, temperature, calcination and mechanism in Light REE and Hea. Chem. Eng. J. 2017, 322, 56–65.

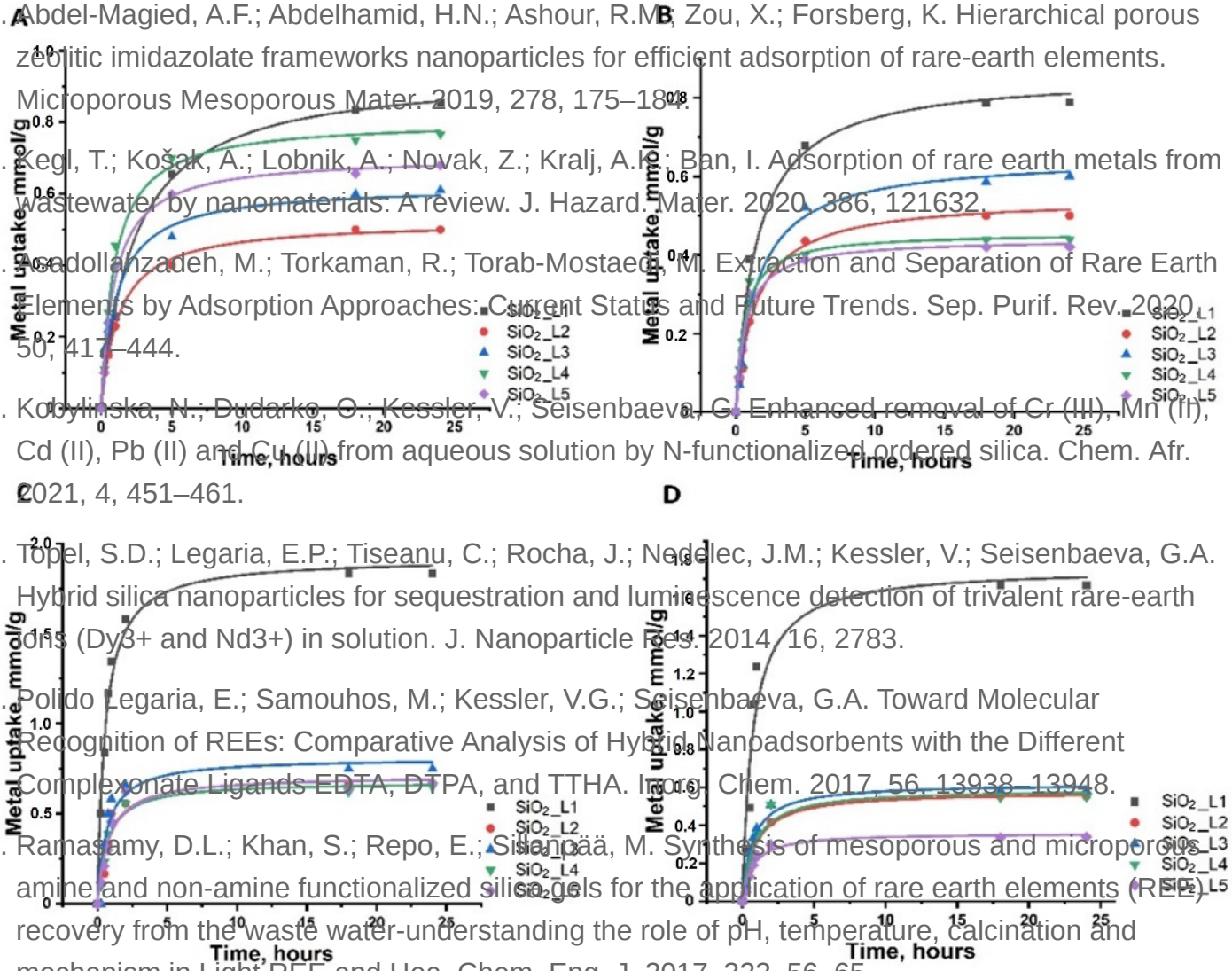

Figure 4. Adsorption kinetics of (**A**) Sm, (**B**) Nd, (**C**) Co and (**D**) Ni onto functionalized silica nanoparticles.

28. Nolack, C.W.; Perkins, K.M.; Calfura, S.C.; Washburn, N.R.; Dzombak, D.A.; Karamalidis, A.K. Effects of ligand chemistry and geometry on rare earth element partitioning from saline solutions to functionalized adsorbents. ACS Sustain. Chem. Eng. 2016, 4, 5115–5124.
29. Da na, E.; Sayari, A. Adsorption of heavy metals on amine-functionalized SBA-15 prepared by co-condensation: Applications to real water samples. Desalination 2012, 285, 62–67.
30. Inoue, K.; Yoshizuka, K.; Ohto, K. Adsorptive separation of some metal ions by complexing agent types of chemically modified chitosan. Anal. Chim. Acta 1999, 388, 209–218.
31. Repo, E.; Kurniawan, T.A.; Warchoł, J.K.; Sillanpää, M.E.T. Removal of Co(II) and Ni(II) ions from contaminated water using silica gel functionalized with EDTA and/or DTPA as chelating agents. J. Hazard. Mater. 2009, 171, 1071–1080.
32. Cegłowski, M.; Schroeder, G. Removal of heavy metal ions with the use of chelating polymers obtained by grafting pyridine-pyrazole ligands onto polymethylhydrosiloxane. Chem. Eng. J. 2015, 259, 885–893.

3. Selectivity and Desorption Tests with Functionalized SiO_2 Nanoparticles

EDS spectroscopy was used to analyze the composition of SiO_2 NPs with different functional groups after adsorption tests with mixtures of metal ions (Nd/Ni, Co/Sm and Ni/Co). Although this technique is able to provide only surface and local information for dense samples, for nano powders such as those used in this work, EDS with its penetration depth of about 1 µm and spot size not less than 100 nm actually provides averaged information about the volume of the material. For most of the samples, researchers could clearly observe selectivity towards a specific metal ion. Thus, for example, SiO_2 with ligand **L1** (**SiO_2_L1**) demonstrated high selectivity towards Ni ions both in the mixture with REEs and with Co ions. On the other hand, both **SiO_2_L2** and **SiO_2_L3** had better selectivity towards Co ions. These results were actually quite unexpected and exciting. The provided functions were supposed to reveal enhanced affinity to LTM, but the experimental results confirmed this supposition only for **L1**, and not **L2**–**5**. The factor that might have been underestimated in building the adsorbent surface is the

potential distance between the functions, derived by the grafting density on the silica surface. As earlier studies of molecular sorbents have indicated, the distance between the coordination sites for ligand fixation is common only in the range 5.3–6.6 Å [40], limiting the availability of adsorption sites for especially smaller cations. Higher ligand grafting of **L1** under the applied reaction conditions favored coordination of Ni^{2+} not only via the ethylene diamine site, but probably also via higher ligand density. The lower ligand density for other ligands may have contributed to better adsorption of REE. This was confirmed by grafting the ligands after acid pre-treatment of SiO_2 NPs, which led to denser functionalized NPs in case of **L3** and **L5**. Subsequent adsorption and selectivity experiments showed that the affinity of these ligands shifted towards LTM by achieving higher maximum capacities and molar ratios for Co (in the case of **SiO_2_L3**) and Ni (in the case of **SiO_2_L5**).

Table 3. Molar ratios of Co and Ni against Sm and Nd by EDS analysis.

Sample	Ni/Nd	Co/Sm	Ni/Co
SiO_2_L1	5.1:1	1:1.65	3.5:1
SiO_2_L2	1:1.78	1:12	1.6:1
SiO_2_L3	1:1	1:18	1:1
SiO_2_L4	1.33:1	1:18	1.85:1
SiO_2_L5	1:3	1:1	1.85:1
SiO_2_L3_acid	1:2.5	6:1	1.3:1
SiO_2_L5_acid	15:1	6:1	2.75:1

Desorption tests were performed with 1 M nitric acid in 50 mL Falcon tubes. After adsorption experiments, the samples were centrifuged and 20 mL nitric acid was then added. The tubes were placed on a shaker for 24 h. Afterwards, the nanoparticles were separated by centrifugation (7000× *g*) and the supernatant was collected, neutralized with ammonia, and titrated with EDTA to determine the desorbed metal amount. The results showed that good desorption rates (85–90%) were achieved with all metal ions. Reusability of these NPs was also tested after three cycles of adsorption and desorption of selected metals (Ni and Sm). Desorption was performed using 1 M nitric acid in 50 mL Falcon tubes, mixing the samples for 24 h on a shaker. Afterwards, the samples were centrifuged (7000× *g*), and the supernatant collected, neutralized with ammonia to pH = 6.5, and titrated with EDTA to calculate the amount of desorbed metal. After desorption, the samples were placed in 10 mL metal solutions (Co and Sm respectively) with a final metal concentration of 20 mM. All the samples showed good desorption rates in each cycle ranging between 70 and 100%. A small decrease in adsorption rates was noticed after the second desorption cycle, especially for **L2** and **L4**; however **L1**, **L3** and **L5** had good adsorption/desorption rates even after three cycles for both metals.

33. Yanovska, E.S.; Vretik, L.O.; Nikolaeva, O.A.; Polonska, Y.; Sternik, D.; Kichkiruk, O.Y. Synthesis and Adsorption Properties of 4-Vinylpyridine and Styrene Copolymer In Situ Immobilized on Silica Surface. Nanoscale Res. Lett. 2017, 12, 2–7.

34. Matveichuk, Y.V.; Rakhman'ko, E.M.; Yasinetskii, V.V. Thiocyanate complexes of d metals: Study of aqueous solutions by UV, visible, and IR spectrometry. Russ. J. Inorg. Chem. 2015, 60, 100–104.

35. Tomina, V.V.; Mel'Nik, I.V.; Pogorilyi, R.P.; Kochkodan, V.M.; Zub, Y.L. Functionalization of the surface of ceramic membranes with 3-mercaptopropyl groups using the sol-gel method. Prot. Met. Phys. Chem. Surf. 2013, 49, 386–391.

36. Manousi, N.; Kabir, A.; Furton, K.G.; Zachariadis, G.A.; Anthemidis, A. Multi-Element Analysis Based on an Automated On-Line Microcolumn Separation/Preconcentration System Using a [illegible]

37. [illegible] heavy [illegible]

38. [illegible] ethod as [illegible]

39. [illegible] th functionalized organic monolayers for selective adsorption of heavy metal ions. Chem. Commun. 2000, 15, 1145–1146.

40. Polido Legaria, E.; Topel, S.D.; Kessler, V.G.; Seisenbaeva, G.A. Molecular insights into the selective action of a magnetically removable complexone-grafted adsorbent. Dalton Trans. 2014, 44, 1273–1282.

41. Park, H.J.; Tavlarides, L.L. Adsorption of neodymium(III) from aqueous solutions using a phosphorus functionalized adsorbent. Ind. Eng. Chem. Res. 2010, 49, 12567–12575.

42. Galhoum, A.A.; Mahfouz, M.G.; Abdel-Rehem, S.T.; Gomaa, N.A.; Atia, A.A.; Vincent, T.; Guibal, E. Diethylenetriamine-functionalized chitosan magnetic nano-based particles for the sorption of rare earth metal ions. Cellulose 2015, 22, 2589–2605.

43. Aghayan, H.; Mahjoub, A.R.; Khanchi, A.R. Samarium and dysprosium removal using 11-molybdo-vanadophosphoric acid supported on Zr modified mesoporous silica SBA-15. Chem. Eng. J. 2013, 225, 509–519.

44. Ettehadi Gargari, J.; Sid Kalal, H.; Shakeri, A.; Khanchi, A. Synthesis and characterization of Silica/polyvinyl imidazole/H2PO4-core-shell nanoparticles as recyclable adsorbent for efficient scavenging of Sm(III) and Dy(III) from water. J. Colloid Interface Sci. 2017, 505, 745–755.

45. He, H.; Gan, Q.; Feng, C. Preparation and application of Ni(ii) ion-imprinted silica gel polymer for selective separation of Ni(ii) from aqueous solution. RSC Adv. 2017, 7, 15102–15111.